BNL-77817-2007-JA

AN ACOUSTIC METHOD FOR MEASURING THE SOUND SPEED OF GASES OVER SMALL PATH LENGTHS

J. S. Olfert
Atmospheric Sciences Division, Brookhaven National Laboratory, Upton, NY 11973-5000

M. D. Checkel and C. R. Koch
Department of Mechanical Engineering, University of Alberta, Edmonton, Canada, T6G 2G8

Submitted for publication in
Review of Scientific Instruments

February 2007

Environmental Sciences Department/Atmospheric Sciences Division

Brookhaven National Laboratory
P.O. Box 5000
Upton, NY 11973-5000
www.bnl.gov

Title

An acoustic method for measuring the sound speed of gases over small path lengths.

Authors

Olfert, J.S.*, Checkel, M.D., and Koch, C.R.

Department of Mechanical Engineering, University of Alberta, Edmonton, Canada, T6G 2G8.

Abstract

Acoustic "phase shift" methods have been used in the past to accurately measure the sound speed of gases. In this work, a phase shift method for measuring the sound speed of gases over small path lengths is presented. We have called this method the discrete acoustic wave and phase detection (DAWPD) method. Experimental results show that the DAWPD method gives accurate (±3.2 m/s) and predictable measurements that closely match theory. The sources of uncertainty in the DAWPD method are examined and it is found that ultrasonic reflections and changes in the frequency ratio of the transducers (the ratio of driving frequency to resonant frequency) can be major sources of error. Experimentally it is shown how these sources of uncertainty can be minimized.

Keywords

Sound speed sensor, gas concentration sensor, gas temperature sensor.

* Current Address: Atmospheric Science Department, Brookhaven National Laboratory, Upton, NY, 11973, USA. *E-mail*: jolfert@bnl.gov

1. Introduction

Ultrasonic gas sensors that measure sound speeds have a number of useful applications in industry such as measuring gas composition, temperature, and flow rates. In particular the authors are concerned with measuring the sound speed of gases in automotive applications, such as measuring the exhaust gas recirculation (EGR) in combustion engines and the quality of gaseous fuels for alternative fueled vehicles (such as hydrogen, natural gas, and propane). In automotive applications sensors must be compact, robust, fast, and cost effective.

Various acoustic methods have been used in the past to measure sound speeds in gases. One of the most common of these methods is based on "time-of-flight" measurements [1-4], where the average sound speed of the medium is measured by sending an ultrasonic pulse between two transducers separated by a known distance, where the sound speed is the found by dividing the distance between the transducers by the time it takes for the pulse to travel across the distance. The time-of-flight method can be quite accurate over long path lengths; however, over short path lengths a number of uncertainties become important. Due to the resonant nature of ultrasonic transducers, a number of pulses are required to fully excite the transducers and it is often unclear which pulse was the first pulse to excite the receiving transducer. Also, as path lengths become smaller, higher accuracy time circuits are required to correctly measure the time-of-flight. Furthermore, the response time of time-of-flight methods are limited by the 'dead-zone' [5] - the minimum time interval between sending wave pulses as determined by the build-up and ringing of the transducers.

The acoustic resonance technique can be used to accurately measure the sound speed of gases in small volumes [6-9]. The acoustic resonance technique is based measuring the acoustical resonance of a volume filled with a gas using ultrasonic transducers. This method can be very sensitive and accurate; however, the response time of the sensor is limited by the rate at which a gas sample can be introduced and fully removed from the resonant volume. Using a resonance technique, Dong et al. [9] developed a sensor to detect hydrogen in air with a response time on the order of 1-2 seconds.

An acoustic phase shift method is a very sensitive method for measuring sound speeds of gases. The phase shift method measures the phase difference between a continuously transmitted and received ultrasonic wave, where the phase difference between the waves is a function of the sound speed. Tinge et al. [10] used this method, with a path length of 240 mm, to accurately measure the composition of binary gas mixtures. More recently, Huang et al. [11] used this method to accurately measure the temperature of air with a path length of 50-100 mm. The advantage of the phase shift method is that, theoretically, the method could use very small path lengths (on the order of one wavelength), and still have high accuracy. Also, since the measurement is continuous very fast response times are possible. Theoretically, a phase shift sensor with 40 kHz transducers with a path length of 10 mm could respond to a step change in sound speed of 350 m/s to 1000 m/s in approximately 11 μs. Furthermore, since the phase shift method can use common ultrasonic piezoelectric transducers, a production sensor could be cost-effective and robust.

The purpose of this paper is to show that the phase shift method can be used to measure the sound speed of gases over path lengths on the order of one wavelength. For clarity we have called this method the discrete acoustic wave and phase detection (DAWPD) method. It will be shown that reflections within the sensor and changes in the frequency ratio of the transducers (the ratio of driving frequency to resonant frequency) can be a major source of error in the DAWPD method. However, these uncertainties can be minimized or corrected and the DAWPD method can be used to accurately measure the sound speed of gases with small path lengths. Previously the authors have used the DAWPD method to accurately measure exhaust gas recirculation concentration in internal combustion engines [12] and gaseous fuel quality for fuel cell vehicles, natural gas vehicles, and variable gaseous fuel vehicles [13]. The purpose of this paper is to describe the DAWPD method and experimentally show the sources of uncertainty in the method (reflections and resonant frequency changes) and show that these uncertainties can be minimized or corrected for.

2. Discrete Acoustic Wave and Phase Detection Method

The DAWPD method measures the phase difference between a transmitted and received ultrasonic wave, where the phase difference between the waves is a function of the sound speed. Figure 1 shows a schematic diagram of the system. The frequency generator produces a continuous square wave (which matches the resonant frequency of the piezoelectric transducers), which drives the piezoelectric transmitter. The piezoelectric transmitter converts the electrical signal into an ultrasonic vibration that travels through the gas medium and is received by the piezoelectric receiver. Likewise, the receiver converts the ultrasonic signal into an electric signal that is amplified and conditioned into a square wave. The square wave produced by the frequency generator and the square wave produced by the receiver are fed into a phase discriminator which produces a voltage which is proportional to the phase difference between the sent and received waves.

An example of a simple and cost effective phase discriminator is an exclusive OR (EXOR) gate. The output of the EXOR has a value of one for two inputs where one of the inputs has a value of one; but for two inputs of zero or one, the output is zero. In the application of the DAWPD method the EXOR will have two square waves as inputs and a square wave as an output as seen in Fig. 2. The output of the EXOR gate (Fig. 2c) goes high if the transmitted signal (Fig. 2a) or the received signal (Fig. 2b), (which will have a difference in phase, ϕ) goes high but not both. Thus as the sound speed increases, the phase difference will decrease; which changes the duty cycle of the EXOR output. The EXOR output is then integrated to give a voltage proportional to the phase difference (Fig. 2c).

The sound speed of the gas medium is a function of the phase difference between the sent and received waves:

$$c = \frac{1}{\frac{\phi}{2\pi fd} + \frac{1}{c_{\mathrm{ref}}}}, \tag{1}$$

where c_{ref} is the sound speed in a reference gas, d is the path length between the speaker and microphone, f is the frequency of the ultrasonic sound wave and ϕ is the phase difference between the two waves.

The advantage of a phase detection method is that a very small sensor can be highly sensitive. The ideal path length of the sensor is determined by the sound speeds to be measured, the phase range of the phase comparator and the driving frequency of the ultrasonic transducers. The ideal path length, or the path length for maximum sensitivity, between ultrasonic transducers can be calculated by:

$$d_{ideal} = \frac{\frac{1}{f}\frac{\theta}{2\pi}}{\frac{1}{c_1} - \frac{1}{c_2}}, \tag{2}$$

where θ is the phase range of the phase comparator in radians, and c_1 and c_2 are the lowest and highest sound speed that will be measured, respectively. To obtain maximum sensitivity in the sensor, the full range of the phase comparator should be used. For an EXOR gate phase comparator the phase range is π radians. This phase comparator provides a linear voltage for a change in phase up to π radians. If less than the full range of the phase comparator is used then sensor sensitivity will decrease. If the range of the EXOR comparator is exceeded, non-valid measurements will occur. Due to the logic of the EXOR gate, a phase difference of 5π/4 will produce the same voltage output as a phase difference of π/4. Therefore it is imperative not to exceed the phase range of the EXOR comparator. Equation 2 is a useful equation for the design of a DAWPD sensor. By changing sensor parameters, such as frequency and phase comparator range, the ideal distance will change. For example, by increasing the driving frequency of the transducers the distance between the transducers should be lessened to retain maximum sensitivity. Therefore, a very small sensor can be manufactured which has excellent sensitivity.

2.1 Uncertainty in the DAWPD method

Although, theoretically, the uncertainty in the DAWPD method is nearly independent of path length, measurement error can arise from other sources. In particular sources of uncertainty in the DAWPD measurement method come from two major sources: 1) ultrasonic reflections within the sensor, and 2) resonant frequency changes of the ultrasonic transducers.

2.1.1 Reflections as a source of uncertainty

An important cause of uncertainty with the DAWPD method is error in the phase measurement caused by ultrasonic reflections within the sensor. Reflections from the interior walls of the sensor and between the transducers cause constructive and destructive interference of the primary ultrasonic wave which alters the phase difference of the received wave. Figure 3 depicts an example of a reflection which causes a change in the phase difference of the received wave. Figures 3a and 3b show the primary transmitted wave and the reflected wave, respectively. The reflected wave (which has reflected off a wall for example) will have travelled a longer path length, will have a smaller amplitude and will be out of phase of the primary wave. The addition of the ultrasonic waves at the position of the receiving transducer will result in a wave of different amplitude and phase of that of the primary transmitted wave, as seen in Fig. 3c. In this particular case the addition of the primary and reflected wave resulted in a received wave of increased amplitude and decreased phase difference compared to the primary wave. The change of phase is proportional to the relative amplitude of the reflected wave and the relative phase difference between the primary and reflected wave. For example, if the amplitude of the reflected wave is small compared to the primary wave, then the change in phase difference will be small, thereby reducing the error in the sensor. Also, when the reflected wave has a phase difference of $0, \pi, 2\pi...$ then the change in phase difference will be zero. However, at a phase difference of $\pi/2, 3\pi /2, 5\pi /2...$, the change in phase difference will be a maximum. This theory shows that the uncertainty is proportional to the amplitude of the reflected wave. By reducing the amplitude of the reflected waves with in the sensor, the uncertainty of the sensor can be reduced.

2.1.2 Frequency ratio deviation as a source of uncertainty

Another cause of uncertainty in the DAWPD method is resonant frequency deviation of the ultrasonic transducers. The excitation of the transmitting transducer and the reception of the ultrasonic signal by the receiving transducer is analogous to the forced harmonic vibration of a damped single degree of freedom spring mass system. In such a system, the phase, ϕ, can be shown to be [14]:

$$\phi = \tan^{-1}\left(\frac{2\zeta(f/f_{\mathrm{n}})}{1-(f/f_{\mathrm{n}})^2}\right), \tag{3}$$

where f is the oscillating frequency, f_{n} is the resonant frequency of the system, and ζ is the damping factor which is defined as the ratio of the damping constant to the critical damping constant. Note that the phase is only a function of the frequency ratio, f/f_{n}, and the damping factor, where a frequency ratio of 1 is the resonant frequency. Equation 3 can be plotted as shown in Fig. 4. From the phase diagram it is apparent that as the forcing frequency deviates from the resonant frequency a phase change will occur which will cause error in the DAWPD method. The DAWPD uses ultrasonic transducers continually driven at a fixed frequency. It is known that age and temperature effects can change the resonant frequency of the transducers. If a DAWPD sensor with temperature dependant resonant frequency transducers is used in an environment where the temperature varies, then the frequency ratio will deviate. This deviation will cause an unwanted phase change in addition to the phase change caused by a change in the sound speed. To avoid this error the following solutions maybe used: i) using resonant frequency matching in a feed back system, ii) using broadband transducers driven away from resonance or

iii) by maintaining the temperature of the transducers. The experimental results will show that by using resonant frequency matching or by maintaining the temperature of the transducers the error caused by resonant frequency changes can be adequately reduced.

3. Experimental Set-Up

The DAWPD prototype was developed to show that suitable sensor accuracy could be achieved with path lengths on the order of one wavelength. A schematic of the DAWPD prototype (with exterior dimensions of 57 mm x 92 mm x 47 mm) is shown in Fig. 5. When the phase shift method is used with such a small path length, reflections can be major source of error. In the DAWPD prototype sensor, accuracy can be achieved by reducing the intensity of the reflections: i) from the walls of the sensor and ii) between the transducers. In the prototype sensor, Kaowool® acoustic insulation, 10 mm thick, was installed on the inside of the enclosure to dampen acoustic reflections from the walls. To reduce the reflections between the transducers, the transducers can be angled and offset from one another. The prototype was designed to be adjustable in angle, offset and normal distance. The angle between the two piezoelectric transducers can be adjusted by rotating the receiving transducer mount in the slot. The offset distance can be adjusted by moving the receiving transducer mount along the transverse slot. Finally, the normal distance can be adjusted by adding shims to the transmitting transducer mount. Through trial-and-error it was found that a normal distance of 8 mm, an offset distance of 4mm, and an angle of 70^{o}, resulted in a sensor with small errors due to reflections (see Sec. 4). The ultrasonic transmitting and receiving transducers used in the DAWPD prototype were Panasonic models EFR-TQB40KS and EFR-RQB40K5, respectively.

To experimentally test the DAWPD prototype sensor a range of sound speeds were measured by mixing two gases of different sound speeds. For a binary gas mixture of ideal gasses (a mixture of gas 1 and gas 2) the sound speed of the mixture will be:

$$c = \sqrt{\frac{RT(y_1 C_{p1} + (1-y_1)C_{p2})}{(y_1 M_1 + (1-y_1)M_2)(y_1 C_{v1} + (1-y_1)C_{v2})}}, \tag{4}$$

where R is the universal gas constant, T is the temperature, y is the molar or volume fraction, M is the molecular weight, C_p and C_v are the specific heats at constant pressure and volume, respectively. In the experiments shown here gas 1 was nitrogen and gas 2 was hydrogen.

Figure 6 depicts the experimental set-up used to vary the composition of the gas. The two gases were fed into the Dasibi® multi-gas calibrator which contains two mass flow controllers. The Dasibi® calibrator was calibrated for the gases used in the experiments. After the gases are mixed, the mixture of gases flow through the ultrasonic sensor and out into a fume hood.

The sound speed is highly dependant on temperature (see Eq. 4). Therefore temperature was measured using a solid state temperature sensor (Omega AD590) that was mounted inside the prototype to check that the gas temperature did not vary.

Sensor output voltage, temperature, and time difference data were collected by passing various gas mixtures of nitrogen and hydrogen. By displaying the transmitted and received signals on the oscilloscope the time difference between the transmitted and received waves could be measured manually.

4. Experimental Results

The concept of the DAWPD measurement method was tested by using a mixture of gases to produce a range of sound speeds. Typical experimental results for the prototype sensor are seen in Figs. 7 and 8. Each figure shows the average of three tests where the error bars represent 2 standard deviations of the experimental data. Figure 7 shows the time difference (Φ) between the transmitted and received signal for various sound speeds. Experimentally, the time difference can be determined by measuring the time difference between the transmitted and received waves on an oscilloscope. Theoretically, the time difference can be found by solving Eq. 1 for the phase difference and knowing that the phase difference is related to the time difference by:

$$\Phi = \frac{\phi}{2\pi f}. \tag{5}$$

With this equation the experimental data can be compared to the theoretical curve as shown in Fig. 7. The figure clearly shows that the experimental data and the theoretical curve agree well.

The calibration curve of the prototype DAWPD sensor is shown in Fig. 8. The static characteristics, such as accuracy, repeatability error, calibration error, and resolution error of the prototype sensor can be found. These static characteristics were calculated and are summarized in Table 1. For each type of error the most conservative, or worst case, error limit was used. Therefore, the maximum error measured for each characteristic is given. The accuracy, or the total error (δ_{total}), of the sensor can be calculated by using the `root sum of squares' of the calibration, repeatability, and resolution error. The accuracy of the sensor was determined to be ±3.2 m/s.

The above work has shown that the DAWPD method can accurately measure sound speeds when ultrasonic reflections are minimized and where there is no change in the frequency ratio of the transducers. As discussed above, reflections within the sensor and frequency ratio changes can theoretically be a major source of error in the DAWPD method. Experimental data shows that reflections within the sensor and frequency ratio changes are a major cause of error. In the following sections, typical experimental results are shown where reflections and frequency ratio changes cause major error in the sensor.

4.1 Experimental results with reflections causing error

Experimental results support that reflections within the sensor is a major cause of sensor error. The prototype sensor described above was tested at a shorter path length (6 mm normal distance, 4 mm offset, and 70^{o} angle), where reflections between the transducers would be more intense. Figure 9a shows the calibration curve of the test and the figure shows that there is considerable deviation from the 'best fit' curve. Figure 9b shows that the peak-to-peak amplitude of the received signal increases and decreases as the sound speed changes. It is probable that the amplitude change is due to the constructive and destructive interference of the primary ultrasonic wave and other reflected sound waves since ultrasonic waves will reflect off the sensor walls and between the transducers and will be received by the receiving transducer. Figure 9c shows that the error from the calibration signal is related to the deviation from the average amplitude. Recall that the amplitude of the received wave will be a maximum when the primary wave and the reflected wave are in phase and likewise the amplitude will be a minimum when the waves are $n\pi$ radians out of phase, where n is an integer (see Sec. 2.1.1). At these two points the phase change, and therefore the error due to reflections, will be zero. By the same argument, the error due to reflections will be a maximum when the amplitude of the received wave is at its average value. This can be seen in Fig. 9c, at values of c ≈ 365 m/s and 410 m/s, where the amplitude of the received signal is near its maximum and minimum value and the error from the calibration curve is near zero.

4.2 Experimental results with resonant frequency changes causing error

As shown in section 2.1.2 resonant frequency changes of the ultrasonic sensors used in a phase shift method (such as the DAWPD method) will cause error in measurement system. In this section the effect of resonant frequency changes in the ultrasonic transducers used in the prototype sensor will be examined. It will be shown that: i) the transducers used in the prototype are highly resonant and their resonant frequency is temperature dependant, ii) frequency ratio changes can cause major errors and iii) by using resonant frequency matching these errors can minimized.

The resonant characteristics of the transducers were tested by varying the driving frequency of the ultrasonic transmitter in the prototype at constant temperature in air. The amplitude of the received wave and the phase shift for each frequency was recorded. Figure 10 shows the frequency response curve for the pair of transducers. From this figure it is apparent that these transducers are highly resonant since the amplitude decay from resonance is so steep. The quality of resonance can be described by the mechanical 'Q' factor, Q_{m}, which can be defined by the relation [15]:

$$Q_{\mathrm{m}} = \frac{f_{\mathrm{n}}}{f_2 - f_1}\,, \tag{6}$$

where f_1 and f_2 are the frequencies on each side of the resonant frequency, f_{n}, where the amplitude is equal to $1/\sqrt{2}$ of the maximum amplitude which occurs at f_{n}. From Eq. 6 it can be shown that Q_m for the transducers used was 115, which is relatively high. The transducers used are of the piezoceramic variety, which are known to have high Q_m factors compared to other kinds of ultrasonic transducers [5]. MEMS (Micro Electro Mechanical System) transducers have been made which have a broader bandwidth, these transducers have been known to have Q_m factors of approximately 10 [16,17]. Transducers with large bandwidths have the advantage of being able to operate at a wider range of frequencies away from the resonant frequency.

Another important transducer characteristic is the phase angle response curve. As mentioned in Sec. 2.1.2, a change in the frequency ratio (the ratio of driving frequency to resonant frequency) of the ultrasonic transducers will cause an undesirable phase shift in the sensor. Figure 11 shows the phase angle response curve of the transducers where the experimental data has been fit with Eq. 3 using a least squares method. From the data fit the damping factor, ζ, was determined to be 0.005. The slope of the curve near resonance is steep (smaller values of ζ correspond to higher slopes at resonance; see Fig. 4), which means that a small change in frequency ratio will result in a large error. Frequency ratios changes can occur from changes in the driving frequency due to changes in the driving electronics (thermal effects etc.) or, more importantly, frequency ratio changes can results from changes in the resonant frequency of the transducers due to ageing or temperature effects.

The effect of temperature on the transducers' resonant frequency was determined experimentally. The resonant frequency of the transducers was found over a range of temperatures using warmed air instead of mixtures of nitrogen and hydrogen and is shown in Fig. 12. The figure shows that the resonant frequency decreases with an increase in temperature and that there is a strong temperature dependence on the resonant frequency of the transducers tested. This would suggest that sound speed measurements made with these transducers using the DAWPD method would have substantial error if the temperature of the gas varied.

The error caused by these temperature dependant transducers can be seen by measuring the sound speed of air at difference temperatures. Recall that an increase in temperature will cause and increase in the sound speed, which for a DAWPD sensor will result in a decrease in the time difference between the sent and received wave. Figure 13 shows the experimental time difference recorded by the prototype DAWPD sensor and the theoretical time difference which would be expected from the sensor. It is apparent that the experimental data without resonant frequency matching does not correspond to the theoretical curve. The cause of this is due to the resonant frequency change of the transducer as the temperature increases. With the current prototype the frequency ratio, f/f_n, will change with temperature since the driving frequency is held constant as the resonant frequency changes. This will cause a phase difference in the sensor as shown in the phase angle response curve (Fig. 11). This phase difference between the transducers causes the transmitted and received signals to shift relative to each other causing measurement error. One method of reducing this error is to adjust the driving frequency of the transmitting transducer to match the resonant frequency of the transducer pair. By matching the driving and the resonant frequency the frequency ratio will remain constant, which will ensure that the phase angle between the transducers remains constant, substantially reducing the error in the system. This method was used and the results are shown in Figure 13. It is clear that matching the frequency greatly increases the accuracy of the sensor, although there is still scatter about the theoretical curve. The cause of the data scatter is due to inaccuracies in manually matching the resonant frequency. Other, more accurate, resonant frequency matching techniques can also be used. One method is to map the frequency response of the transducers to changes in temperature (see Fig.12). The temperature of the transducers can be measured and the driving frequency adjusted to match the resonant frequency of the transducers (although this method doesn't compensate for changes in the resonant frequency due to ageing effects). Commercially, some measurement systems have temperature controlled oscillators or oscillators that are locked to the resonant frequency of the transducers [5,18].

Error due to frequency ratio changes can also be reduced by operating transducers away from resonance. The advantage would be that changes in resonance frequency would not produce a large change in phase angle. Figure 4 shows the theoretical phase angle curve for a damped single degree of freedom spring mass system. It is apparent from the figure that the slope of the phase angle curve is less steep above and below resonance. If a transducer was operated well away from resonance, then changes in the frequency ratio due to temperature or age would have a much smaller effect on the phase of the system, resulting in reduced error due to frequency ratio changes. MEMS devices have lower Q_m factors than piezoceramic devices, making the MEMS devices ideal candidates for a system which operates away from the resonant frequency of the transducers.

7. Summary

The purpose of this paper was to show that the phase shift method can be used to measure the sound speed of gases over small path lengths. We have developed a prototype sensor called the discrete acoustic wave and phase detection (DAWPD) sound speed sensor. The path length of this sensor is on the order of one wave length in air. Such a compact sensor makes it ideal for applications (such as automotive applications) were a small and accurate sound speed sensor is required. It was shown that the DAWPD sensor can accurately measure the sound speed of gas (±3.2 m/s). Furthermore, it was shown that uncertainties in the DAWPD sensor can arise from two major sources: i) ultrasonic reflections within the sensor, and ii) changes in the frequency ratio of the transducers. In the prototype sensor the reflections were reduced by insulating the walls of the sensor and adjusting the offset distance, normal distance, and angle between the transducers. It was also shown that the resonant frequencies of the transducers used in the prototype were highly dependant on temperature and that changes in temperature resulted in large errors in the measurement. In the prototype this error was corrected by manually adjusting the driving frequency to match the resonant frequency of the transducers (i.e. maintaining the frequency ratio at unity). In a commercial sensor this could be more readily achieved by i) using resonant frequency matching in a feed-back system or ii) driving the transducers away from the resonant frequency.

References

1. G. Hallewell, G. Crawford, D. McShurley, G. Oxoby, and R. Reif, “A sonar-based technique for the ratiometric determination of binary gas mixtures," Nuclear Instruments and Methods in Physics Research, vol. A264, pp. 219-234, 1988.

2. G. Hallewell, “A sound method for measurement of gas concentration," Research and Development, pp. 98-101, Sept 1988.

3. J. F. Figueroa and J. S. Lamancusa, “A method for accurate detection of time of arrival: Analysis and design of an ultrasonic ranging system,” J. Acoust. Soc. Am, vol. 91, pp. 486-494, 1992.

4. M. Joos, H. Muller, and G. Linder, “An ultrasonic sensor for the analysis of binary gas mixtures,” Sensors and Actuators B, vol. 15-16, pp. 413-419, 1993.

5. W. Manthey, N. Kroemer, and V. Magori, “Ultrasonic transducers and transducer arrays for applications in air,” Meas. Sci. Technol., vol. 3, pp. 249-261, 1992.

6. S. O. Colgate, C. F. Sona, K. R. Reed, and A. Sivaraman, “Experimental Ideal Gas Reference State Heat Capacities of Gases and Vapors,” J. Chem. Eng. Data, vol. 35, pp. 1-5, 1990.

7. E. Polturak, S. L. Garret, and S. G. Lipson, “Precision acoustic gas analyzer for binary mixtures," Rev. Sci. Instrum., vol. 57, pp. 2837-2841, 1986.

8. F. D. Shields and J. Faughn, “Sound velocity and adsorption in low-pressure gases confined to tubes of circular cross section,” J. Acoust. Soc. Am, vol. 46, pp. 158-163,

1969.

9. S. Dong, F. Bai, J. Li, D. Viehland, “A piezoelectric-sound-resonance cavity for hydrogen gas detection”, IEEE Ultrasonics, Ferroelectrics, and Frequency Control, vol. 50, no. 9, 1105-1113, 2003.

10. J. T. Tinge, K. Mencke, L. Bosgra, and A. A. H. Drinkenburg, “Ultrasonic gas analyser for high resolution determination of binary-gas composition,” J Physics E: Scientific Instruments, vol. 19, pp. 953-956, 1986.

11. K. N. Huang, C. F. Huang, Y. C. Li, and M. S. Young, “High precision, fast ultrasonic thermometer based on measurement of the speed of sound in air,” Rev. Sci. Instrum., vol. 73, no. 11, 4022-4027, 2002.

12. J. S. Olfert and M. D. Checkel, “An ultrasonic sound speed sensor for measuring EGR levels,” Accepted by the Journal of Automobile Engineering, 2006.

13. J. S. Olfert and M. D. Checkel, “A fuel quality sensor for fuel cell vehicles, natural gas vehicles, and variable gaseous fuel vehicles,” Society of Automotive Engineers, 2005. 2005-01-3770

14. W. T. Thomson and M. D. Dahleh, *Theory of Vibration with Applications*. Prentice Hall, Inc., 1998.

15. J. Biltz, *Elements of Acoustics*. Butterworth and Co., 1964.

16. P. D. Harris, M. K. Andrews, and G. C. Turner, “Ultrasonic transmission and reception from bulk-micromachined transducers,” IEEE Transactions on Ultrasonics,

Ferroelectrics, and Frequency Control, vol. 48, no. 1, pp. 224-231, 2001.

17. I. Ladabaum, X. Jin, H. T. Soh, A. Atalar, and B. T. Khuri-Yakub, “Surface micromachined capacitive ultrasonic transducers,” IEEE Transactions on Ultrasonics, Ferroelectrics, and Frequency Control, vol. 45, no. 3, pp. 678-690, 1998.

18. Anon, “Proximity sensor using a single piezoceramic ultrasonic transducer,” IBM Technical Disclosure Bulletin, vol. 29, no. 2, pp. 935-936, 1986.

Table 1: Static characteristics of the DAWPD sound speed sensor

Characteristic	Value (m/s)
Accuracy, δ_{total}	±3.2
Calibration Error	±3.0
Repeatability Error	±1.2
Resolution Error	±0.2
Range of Sound Speeds Tested	350-446

Figure Captions:

Figure 1: Schematic of DAWPD ultrasonic gas sensor.

Figure 2: Phase discrimination of transmitted and received signals.

Figure 3: Interference of the primary and reflected signal and the resulting received signal.

Figure 4: Phase of vibration as a function of the frequency ratio (f/f_n) for various damping factors (ζ)

Figure 5: Schematic of the DAWPD prototype sound speed sensor.

Figure 6: Schematic of experimental set-up.

Figure 7: Experimental results of prototype compared to theoretical curve.

Figure 8: Calibration curve of prototype.

Figure 9: Comparison of error from calibration curve and amplitude of received signal. (Spline curves are added in (c) to guide the eye.)

Figure 10: Frequency response curve for transducers used in the prototype sensor (Panasonic EFR-TQB40KS and EFR-RQB40K5).

Figure 11: Phase angle response curve for transducers used in the prototype sensor (Panasonic EFR-TQB40KS and EFR-RQB40K5). The experimental data is fit with Eq. 3, where ζ was determined to be 0.005.

Figure 12: Temperature dependance of the resonant frequency of the ultrasonic transducers (Panasonic EFR-TQB40KS and EFR-RQB40K5).

Figure 13: Comparison of experimental data with and without resonant frequency matching to the theoretical time difference of sensor output.

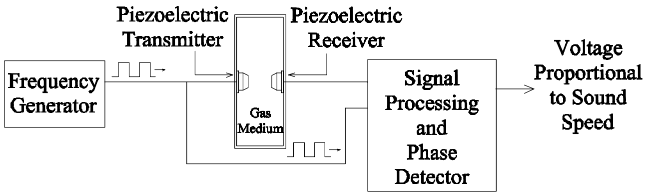
Piezoelectric Transmitter
Piezoelectric Receiver
Frequency Generator
Gas Medium
Signal Processing and Phase Detector
Voltage Proportional to Sound Speed

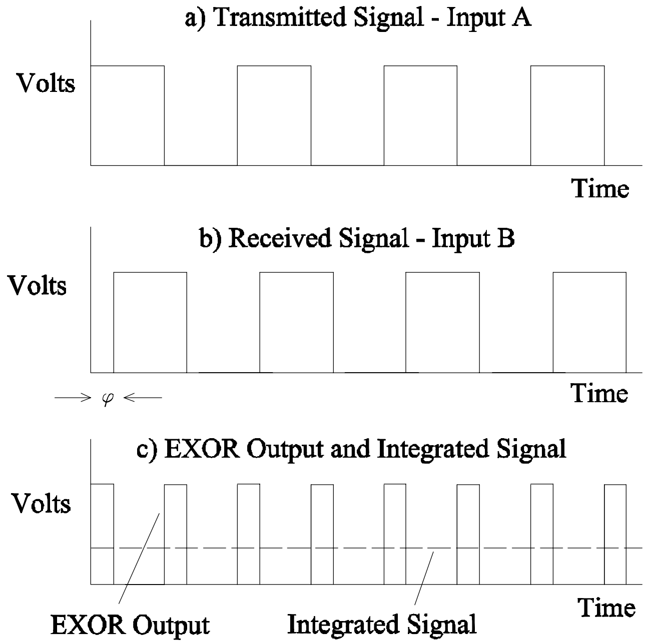
a) Transmitted Signal - Input A
Volts
Time
b) Received Signal - Input B
Volts
φ
Time
c) EXOR Output and Integrated Signal
Volts
EXOR Output
Integrated Signal
Time

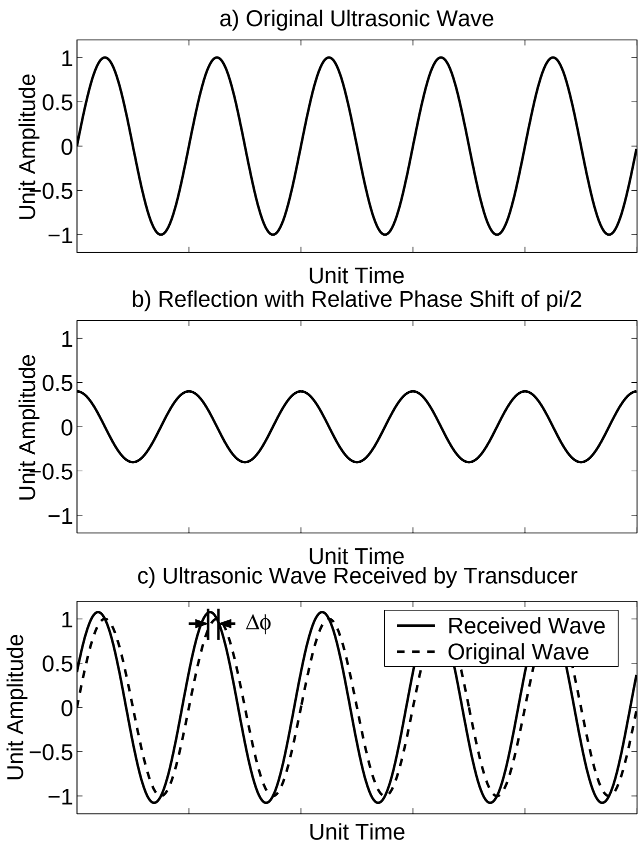

a) Original Ultrasonic Wave
Unit Amplitude
1
0.5
0
−0.5
−1
Unit Time
b) Reflection with Relative Phase Shift of pi/2
Unit Amplitude
1
0.5
0
−0.5
−1
Unit Time
c) Ultrasonic Wave Received by Transducer
Δφ
Received Wave
Original Wave
Unit Amplitude
1
0.5
0
−0.5
−1
Unit Time

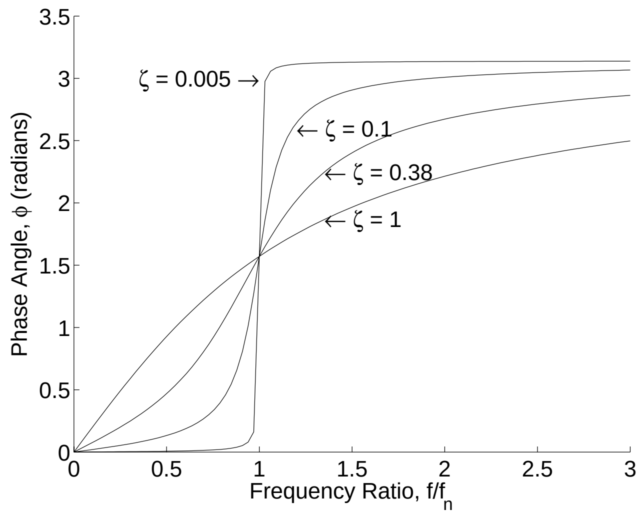

Phase Angle, ϕ (radians)
Frequency Ratio, f/f_n
ζ = 0.005
ζ = 0.1
ζ = 0.38
ζ = 1
0
0.5
1
1.5
2
2.5
3
3.5

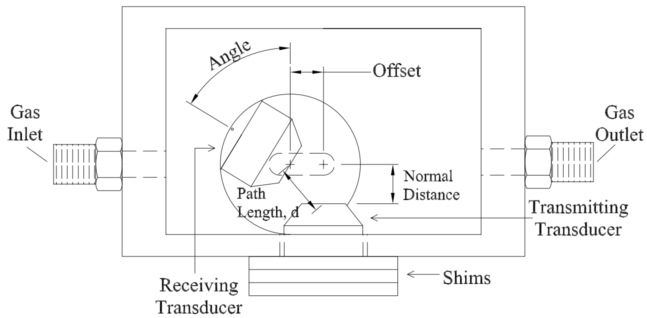
Angle
Offset
Gas
Inlet
Gas
Outlet
Normal
Distance
Path
Length, d
Transmitting
Transducer
Receiving
Transducer
Shims

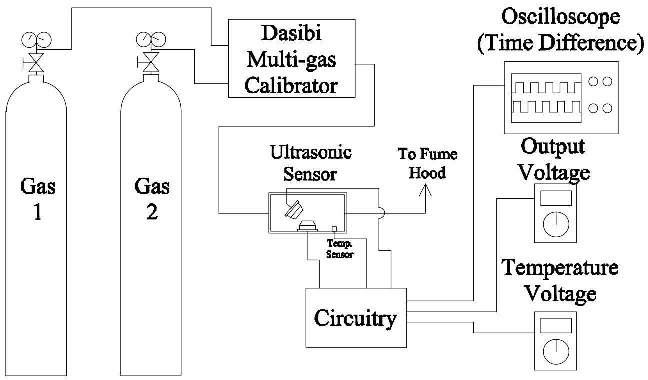
Dasibi
Multi-gas
Calibrator
Oscilloscope
(Time Difference)
Ultrasonic
Sensor
To Fume
Hood
Output
Voltage
Gas
1
Gas
2
Temp.
Sensor
Temperature
Voltage
Circuitry

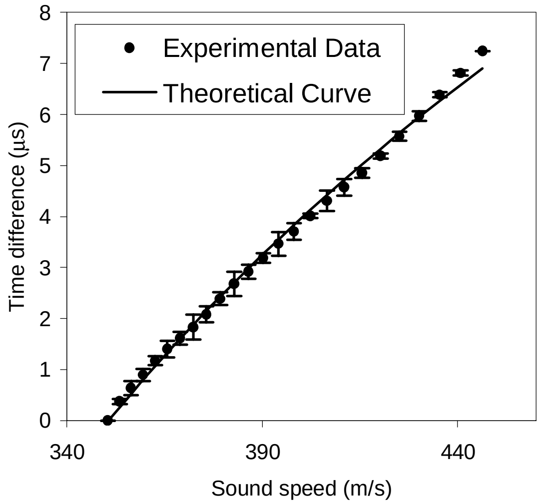

Experimental Data
Theoretical Curve
Time difference (μs)
Sound speed (m/s)
0
1
2
3
4
5
6
7
8
340
390
440

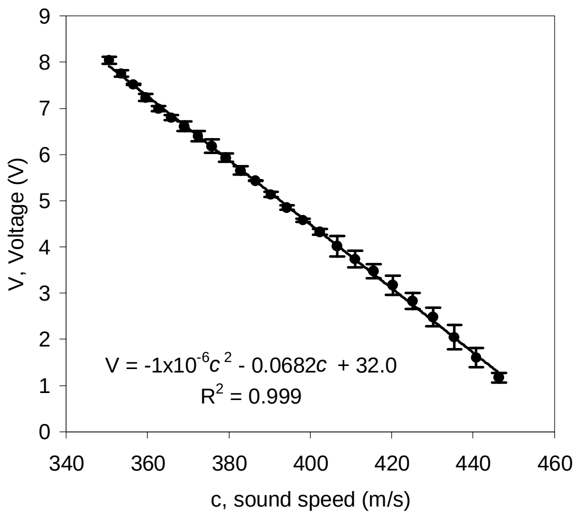

9
8
7
6
5
4
3
2
1
0
V, Voltage (V)
V = -1x10^{-6}c^2 - 0.0682c + 32.0
R^2 = 0.999
340
360
380
400
420
440
460
c, sound speed (m/s)

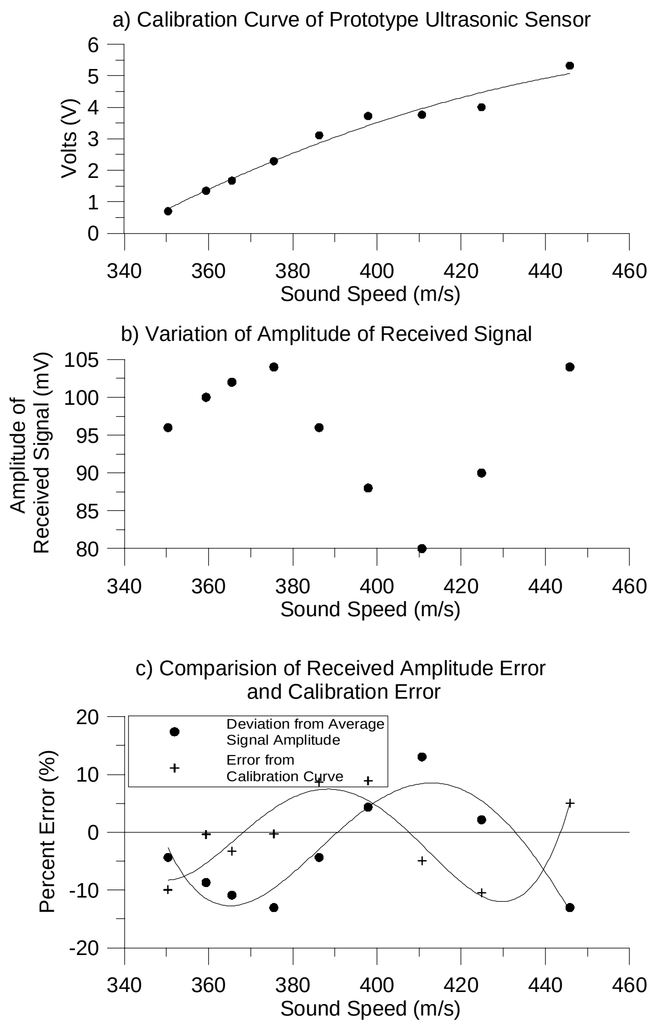

a) Calibration Curve of Prototype Ultrasonic Sensor
Volts (V)
Sound Speed (m/s)
b) Variation of Amplitude of Received Signal
Amplitude of Received Signal (mV)
Sound Speed (m/s)
c) Comparision of Received Amplitude Error and Calibration Error
Deviation from Average Signal Amplitude
Error from Calibration Curve
Percent Error (%)
Sound Speed (m/s)

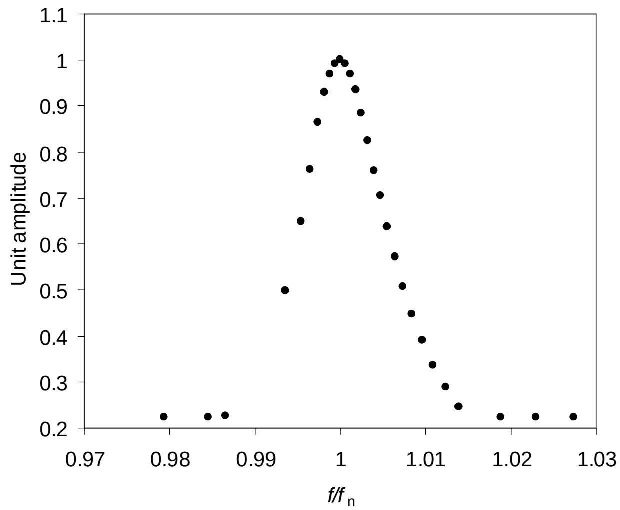

1.1
1
0.9
0.8
0.7
0.6
0.5
0.4
0.3
0.2
Unit amplitude
0.97
0.98
0.99
1
1.01
1.02
1.03
f/f n

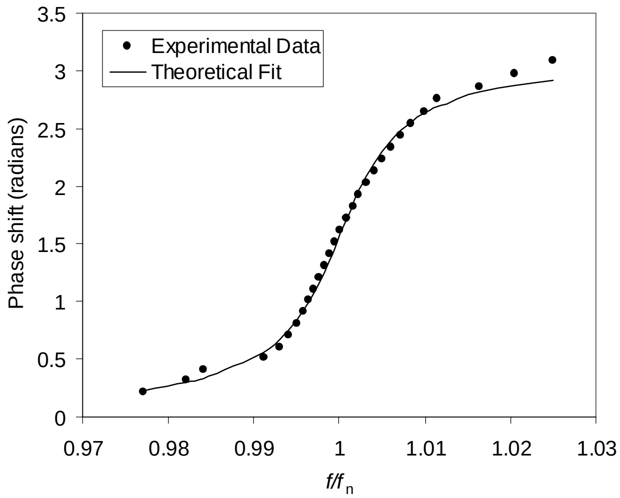
Experimental Data
Theoretical Fit
Phase shift (radians)
3.5
3
2.5
2
1.5
1
0.5
0
0.97
0.98
0.99
1
1.01
1.02
1.03
f/f n

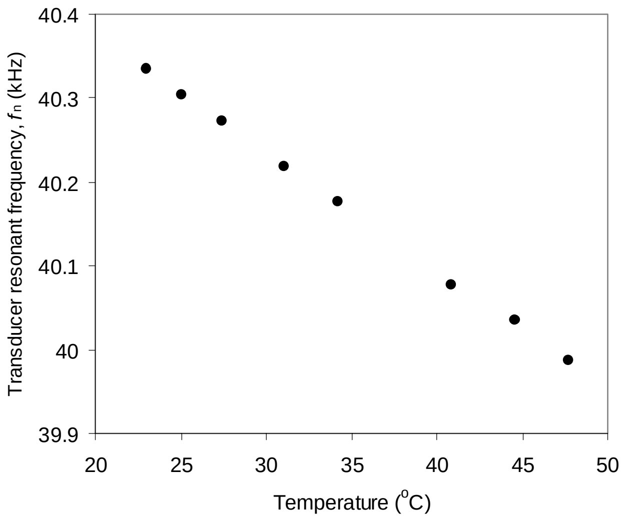

40.4
40.3
40.2
40.1
40
39.9
20
25
30
35
40
45
50
Transducer resonant frequency, f_n (kHz)
Temperature (^{o}C)

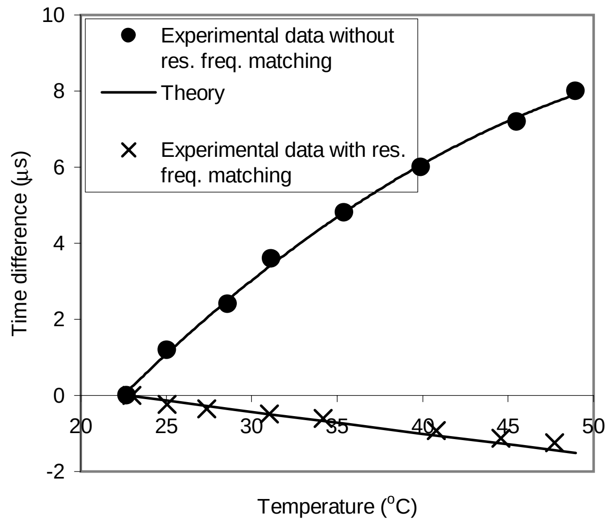

Experimental data without res. freq. matching
Theory
Experimental data with res. freq. matching
Time difference (μs)
Temperature (°C)
10
8
6
4
2
0
-2
20
25
30
35
40
45
50